Full Paper

Wiley Online Library

ELECTROANALYSIS

DOI: 10.1002/elan.201800415

Sensitive Voltammetric Determination of Bisphenol A Based on a Glassy Carbon Electrode Modified with Copper Oxide-Zinc Oxide Decorated on Graphene Oxide

Şükriye Ulubay Karabiberoğlu*[a]

Abstract: A highly sensitive and selective chemical sensor was prepared based on metallic copper-copper oxides and zinc oxide decorated graphene oxide modified glassy carbon electrode (Cu–Zn/GO/GCE) through an easily electrochemical method for the quantification of bisphenol A (BPA). The composite electrode was characterized via scanning electron microscopy (SEM), X-Ray photoelectron spectroscopy (XPS) and electrochemical impedance spectroscopy (EIS). The electrochemical behavior of BPA in Britton-Robinson (BR) buffer solution (pH 7.1) was examined using cyclic voltammetry (CV). Under optimized conditions, the square wave voltammetry (SWV) response of Cu–Zn/GO/GCE towards BPA indicates two linear relationships within concentrations (3.0 nmol L^{-1}–0.1 µmol L^{-1} and 0.35 µmol L^{-1}–20.0 µmol L^{-}) and has a low detection limit (0.88 nmol L^{-1}). The proposed electrochemical sensor based on Cu–Zn/GO/GCE is both time and cost effective, has good reproducibility, high selectivity as well as stability for BPA determination. The developed composite electrode was used to detect BPA in various samples including baby feeding bottle, pacifier, water bottle and food storage container and satisfactory results were obtained with high recoveries.

Keywords: graphene oxide · metallic copper · copper oxides · zinc oxide · Bisphenol A

1 Introduction

Bisphenol A which is also known as BPA (2,2-bis(4-hydroxyphenyl)propane) has been extensively used in the fabrication of polycarbonate, unsaturated polyester, epoxy resin etc. and can be present in the water bottles, plastic food container, infant feeding bottles and etc. The leaching of BPA from these products is very important for human health since BPA is known as an endocrine disruptor [1,2]. It can also cause many problems such as decreasing of sperm quality, increasing of cancer risk by weakening the immune system, diabetes, thyroid disorder etc. [3]. The current tolerable daily intake (TDI) value of BPA has been reported as 4.0 µg/kg bw/day by the European Food Safety Authority (EFSA) in January 2015 [4]. Regarding mentioned points above, development of a convenient, cheap, easy, sensitive and selective analytical method for the BPA determination is an important issue in terms of food security.

Various analytical approaches have been reported in order to monitor the concentration of BPA such as liquid chromatography [5], gas chromatography [6], flow injection chemiluminescence [7], fluorimetry [8] and electrochemical techniques [9–11]. Although chromatographic and spectroscopic techniques are very sensitive and selective, these techniques include time-consuming extraction and sample clean-up steps, as well as require sophisticated and expensive devices. On the other hand; voltammetric techniques are very simple, cost-effective, rapid and do not require sample pretreatment steps. Despite all these advantages, one of the obstacles in voltammetric BPA determination is the relatively high oxidation potential of BPA with poor reproducibility and sensitivity at traditional working electrodes. Additionally, the oxidation products of BPA cause the fouling of the electrode surface which is the major problem occurs during the electrooxidation phenols due to the electropolymerization of phenolic compounds [3,9,10]. In order to overcome these problems, developing novel sensing materials becomes crucial for the sensitive and selective determination of BPA. The bare electrode surface can be modified with various materials including carbonaceous material: graphene derivatives (graphene, graphene oxide (GO), reduced graphene oxide) [9,11–13], carbon nanotubes (CNT) [3,14–16], metal-metal oxide based composites [17–20], conductive polymers [21,22], ionic liquids [23], molecularly imprinted polymers [24], etc. In particular, GO has attracted considerable attention because it can be chemically modified which has a large surface area,

[a] Ş. Ulubay Karabiberoğlu
Ege University
Faculty of Science
Department of Chemistry
35100 Bornova, İzmir Turkey
Tel: +90 232 311 5547
Fax: +90 232 388 8264
E-mail: sukriye.karabiberoglu@ege.edu.tr
sukriyeulubay@gmail.com

Supporting information for this article is available on the WWW under https://doi.org/10.1002/elan.201800415

© 2019 Wiley-VCH Verlag GmbH & Co. KGaA, Weinheim

good mechanical and thermal properties [25]. Moreover, the basal plane and sheet edge of GO surface contain OH, –COOH and epoxides groups which are hydrophilic. Due to the presence of these groups, the GO displays good hydrophilicity and dispersibility in water [26]. Although the GO conductivity is not as high as graphene, it is considered a suitable sensor candidate in electroanalytical applications. Graphene-based composite materials for the determination of BPA have been reported in many studies. For example, Au nanoparticle loaded GO-CNT composite film was fabricated for the sensitive BPA determination with 5.0 nM–100 nM linear range and the detection limit was calculated as 1.0 nM [11]. Deng et al. prepared a molecularly imprinted chitosan-graphene paste electrode with acetylene black for the BPA determination with the detection limit of 6.0 nM [27]. Another study for BPA detection in environmental pollutants was performed with Pt nanoparticles that were functionalized graphene electrode [28]. These papers indicated that the BPA electrooxidation is influenced deeply by the surface modification.

Bimetallic surfaces have been attracting growing attention owing to their electrical, optical and catalytical properties. On the other hand, bimetallic oxide or metal nanoparticles can be easily synthesized with electrochemical methods and it leads to stable surface. However, the bimetallic structures at the electrode surface can be fragile in the absence of stabilizing material. To solve this problem, in the first step, the electrode surface can be modified with some materials which have a higher surface area such as carbon nanotubes, polymers, and graphene-based material. For this purpose, graphene oxide may be used as supporting material allows dispersing of the metal oxides and metal nanoparticles and provides additional electrocatalytic sites. Additionally, the sensitivity and selectivity of the electrode towards target analytes can be increased with the metal oxides and metal nanoparticles on the graphene oxide surface due to combination of good properties of GO and metal oxides and metal nanoparticles [9,13].

As can be deduced from the literature review, there are no reports on the copper oxide-zinc oxide/graphene oxide nanocomposite (Cu–Zn/GO/GCE) for the BPA sensing applications. Here, a novel method, Cu–Zn/GO modified glassy carbon electrode (GCE) was constructed and used for sensitive determination of BPA. The morphological, electrical and structural analysis of the newly synthesized materials were studied by means of SEM, XPS and EIS. The electrochemical behavior of BPA on the Cu–Zn/GO/GCE was studied with the cyclic voltammetry (CV). The square wave voltammetry (SWV) was utilized for quantitative analysis in order to improve sensitivity in BPA analysis under the optimum conditions. The prepared novel sensor offered several advantages such as high sensitivity and selectivity, simple and cheap production. By taking into account all results, it can be concluded that the novel sensor will offer a great opportunity for the determination of BPA in various samples including baby feeding bottle, pacifier, water bottle and food storage containers.

2 Experimental

2.1 Reagents and Solutions

A stock solution of BPA obtained from Sigma Aldrich with purity of $>99\,\%$ ($10.0\,mmol\,L^{-1}$) was prepared in absolute ethanol and stored at $4\,^{\circ}C$. Graphite powder (average particle size <20 micron), sulphuric acid (H_2SO_4), sodium hydroxide (NaOH), hydrochloric acid (HCl), hydrogen peroxide (H_2O_2), potassium permanganate ($KMnO_4$), copper sulphate ($CuSO_4$), zinc sulphate ($ZnSO_4$), alumina (Al_2O_3), acetic acid (CH_3COOH), boric acid (H_3BO_3), phosphoric acid (H_3PO_4), *N,N*-dimethylformamide (DMF) with analytical grade were brought from Sigma-Aldrich Chemical Co. The Britton-Robinson (BR) buffer solution prepared at certain pH ranges was used as a supporting electrolyte in electrochemical measurements. Double distilled water with an electric resistance of 18.2 Mohm.cm was manufactured from Millipore Milli Q system. All electrochemical experiments were performed at room temperature.

2.2 Instrumentation

The voltammetric and electrochemical impedance measurements were performed in an electrochemical cell containing three electrode system which are bare GCE (1.6 mm in diameter) and composite film modified GCE, an Ag/AgCl (sat.KCl) and a Pt wire as working electrode, reference electrode and counter electrode, respectively. Autolab 302 N Electrochemical Analyzer system was used during all electrochemical measurements. CV and SWV were carried out for the investigation of electrochemical behavior and sensing applications of BPA. Spectroscopic measurements for the comparison of BPA detection in various samples were carried out with UV-vis spectrophotometer (PG Instrument, PG 80+ model) at a wavelength of 275 nm using a quartz cell which has optical path length of 1.0 cm. The SEM analyses were carried out using the QuantaTM 250 FEG for the morphological surface characterization of composite electrodes. Thermo Scientific Spectrometer with K-Alpha surface analysis was used for the XPS study of the Cu–Zn/GO/GC composite electrode. The pH measurements were carried out via WTW handheld 330i ion analyzer.

2.3 Preparation of Cu–Zn/GO Modified GCE

Graphene oxide (GO) was synthesized from graphite using an adapted Hummers method [29]. Briefly, about 2.0 g graphite particles were stirred in 50 mL of concentrated H_2SO_4 for 8 h in the ice bath. At the room temperature, the solution mixture was constantly stirred for 2.0 hours and then 7.0 g of $KMnO_4$ was added. After stirring this mixture at $80\,^{\circ}C$ for 45 minutes, 100 mL of

 © 2019 Wiley-VCH Verlag GmbH & Co. KGaA, Weinheim

ultrapure water was added and the temperature was increased to 100 °C. Finally, the reaction was completed by the addition 250 mL of distilled water and 10 mL of 30 % H_2O_2 solution. The final product was centrifuged until the solution pH reaches 7.0 and then, washed with ultrapure water. The obtained solid was dried at 60 °C.

In order to modify the electrode, GO suspension was prepared with 0.04 g graphene oxide in 2.0 mL of DMF. Initially, in order to obtain a mirror-like surface, GCE surface was polished with Al_2O_3 suspensions (0.05–3.0 μm). After rinsing of the electrode with ultrapure water, the electrode was sonicated in ethanol-ultrapure water mixture (1:1) for 3.0 min. In order to provide the modification of GCE surface with GO, 10 μL aliquot of the suspension of GO was dropped onto the GCE surface (GO/GCE). Then, the electrode was kept in the oven at 75 °C for half-hour in order to evaporate the solvent (DMF). Copper oxide-metallic copper particles and zinc oxide particles were loaded on the GO/GCE surface using an aqueous solution of 0.1 M H_2SO_4 containing 1.0 mmol L^{-1} $CuSO_4$ and 1.0 mmol L^{-1} $ZnSO_4$ at −1.40 V for 300 sec. under chronoamperometric conditions. The composite electrode, denoted as Cu–Zn/GO/GCE, was slowly washed with water. For the comparison of the modified electrodes' response towards BPA electrooxidation, copper oxide or zinc oxide was also located on the GO/GCE surface and both were attached on the bare GCE surface via same chronoamperometric technique. Prepared electrode was represented as Cu/GO/GCE, Zn/GO/GCE and Cu–Zn/GCE, respectively.

2.4 Preparation of Real Samples

Four different types of plastic products (baby feeding bottle, pacifier, water bottle and food storage container) were bought from the local market. Firstly, all of them were cut into little pieces, sonicated in acetone and water. Then, 2.0 g of each product were added into ethanol and were heated at 80 °C during 48 h. After cooling the mixture, it was filtrated and then the liquid part was collected in 100 ml of volumetric flask. For the BPA analysis in real samples, 5.0 mL of sample was added to the electrochemical measurement cell containing 5.0 mL of BR buffer solution (pH of 7.1). The analytical performance of Cu–Zn/GO/GCE in real sample solutions were evaluated with the standard addition method.

3 Results and Discussions

3.1 Characterization of the Cu–Zn/GO Modified GCE

The typical morphological analysis of GO/GCE and Cu–Zn/GO/GCE was carried out with the SEM technique. As can be seen form Figure 1A, the GCE surface was covered by graphene oxide with numerous sharp edges nanosheets. These nanosheets in the GO structure both provided an increase in the electrode surface area and roughness and also generated more active sites for the formation of Cu^0–CuO and ZnO on GO surface. The image shows a thin wrinkled paper-like morphology (Figure 1A). A change in surface morphology of the GO structure was observed after the deposition of Cu/CuO–ZnO particles onto the GO surface (Figure 1B–D with different magnitude). These images indicated that Cu/CuO–ZnO particles have been successfully synthesized on the graphene oxide, since particles or flower grains covering the flaky layered structure of the graphene oxide were observed. The Cu^0–CuO and ZnO flowers closely located at the surface of graphene oxide sheets. As a result, the SEM results showed that flower-like Cu–Zn microstructures have been grown successfully on the GO surface.

Further evidence for the component of the developed composite electrode is obtained by the XPS measurement, which is an excellent technique for understanding the oxidation state of the copper and zinc ions on the GO surface. The XPS results are shown in Figure 2. The survey scan of a wide spectral region in Figure 2A indicates that the current elements are on the composite electrode. The survey spectrum of the Cu–Zn/GO/GCE contains C, O, Cu and Zn peaks at definite binding energy values on the Cu–Zn modified GO/GC electrode surface. The deconvoluted XPS C 1s spectrum of composite electrode reveals five components: 284.6 eV (peak 1, sp^2 hybridized carbon), 285.45 eV (peak 2, sp^3 hybridized carbon), 287.41 eV (peak 3, C–O), 287.98 eV (peak 4, C=O), and 289.36 eV (peak 5, O–C=O) (Figure 2B), which can be attributed to the functional groups present on the GO sheets [30–32]. The XPS spectrum of the Cu 2p region is shown in Figure 2C. The Cu 2p spectrum displays Cu $2p_{1/2}$ and Cu $2p_{3/2}$ lines. The peak-fit of Cu $2p_{3/2}$ revealed two peaks at 932.70 eV and 933.79 eV which may be related to Cu^0 and Cu^+) and Cu^{2+} [(CuO or $Cu(OH)_2$] respectively. On the other hand, the Cu $2p_{1/2}$ core level signal at 952.45 eV can be assigned to CuO form on the surface [33–36]. These results indicate that Cu^0, Cu^+, Cu^{2+} species were formed on the GO surface. As in the case of Zn 2p, two characteristic peaks of $Zn_{3/2}$ (1022.54 eV) and $Zn_{1/2}$ (1045.61 eV) were observed (Figure 2B). The difference between the two binding energies of Zn 2p is 23.07, which is in agreement with the reference value of bulk ZnO. In particular, the peak at 1022.54 eV is related to Zn^{2+} in the ZnO structure on the GO surface [37,38]. As can be understood from these data, copper and zinc species are deposited on graphene oxide as Cu^0, CuO or $Cu(OH)_2$ and ZnO species. For ease of notation, the composite electrode will be denoted as Cu–Zn/GO/GCE in the subsequent parts of the study. From the XPS quantitative analysis data, the atomic percentage of modified electrode surface was obtained as Cu: 5.25 %, Zn: 2.82 %, C: 56.13 %, O:34.33 %, S: 0.55, N: 0.92.

EIS was used for the further characterization of electronic properties of bare and metal oxide-graphene oxide composite electrodes. Nyquist plots (Figure 3) were obtained for at all electrodes using 5.0 mmol L^{-1} $K_3[Fe(CN)_6]/K_4[Fe(CN)_6]$ redox probe system in

 © 2019 Wiley-VCH Verlag GmbH & Co. KGaA, Weinheim

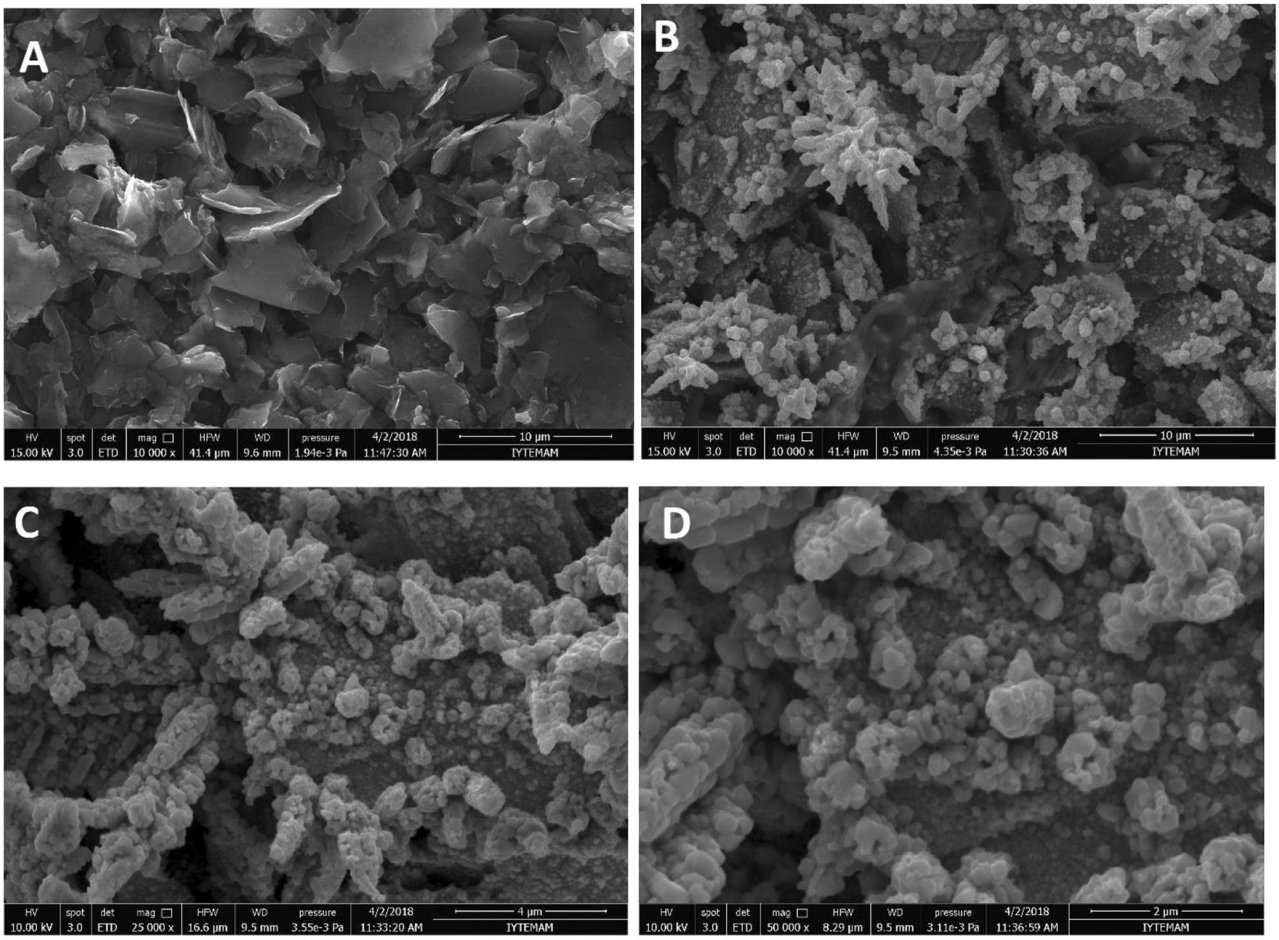

Fig. 1. SEM images of (A) GO/GCE, (B) Cu–Zn/GO/GCE with x10000 magnitude, (C) Cu–Zn/GO/GCE with x25000 magnitude, (D) Cu–Zn/GO/GCE with x50000 magnitude.

0.1 mol L^{-1} KCl solution with the frequencies range from 0.05 to 75,000 Hz and 0.05 V of amplitude. The EIS data were fitted in order to obtain equivalent circuit containing charge transfer resistance (R_{ct}), electrolyte resistance (Rs), Warburg impedance (W) and the double layer capacitance (C_{dl}) (Figure 3B-inset). The Rct value of 849 ohm at bare GCE indicated that a slow electron transfer between the electrode interface and redox probe occurred. The lowest R_{ct} value (113 Ω) for the Cu–Zn/GO/GCE indicated a relatively fast charge transfer when compared with the GO/GCE (410 Ω), Cu/GO/GCE (246 Ω), Zn/GO/GCE (203 Ω) and Cu–Zn/GCE (640 Ω). As can be followed from the Figure 3, the best electrical conductivity was obtained at Cu–Zn/GO/GCE and the presence of metal oxides and GO accelerated the electron transfer between redox probe and electrode surface and exhibit electro-conductibility due to synergetic action graphene oxide and metal oxides. Thus it can be concluded that, Cu^0–CuO and ZnO were successfully loaded on the GO sheets.

The effective surface areas (EASA) of all used electrodes were calculated in 1.0 mmol L^{-1} $K_4Fe(CN)_6$ + 0.1 mol L^{-1} KCl solution by Randles-Sevcik equation [39,40]:

$$I_p = (2.69 \times 10^5) n^{3/2} A D^{1/2} C^* v^{1/2} \quad (1)$$

Here; Ip is the peak current (A), n is the (n = 1) electron numbers in redox reaction, D is the diffusion coefficient (6.7×10^{-6} $cm^2 s^{-1}$ at 25 °C), A is the electro-active surface area (cm^2), C^* is the concentration of $K_4Fe(CN)_6$ (1.0 mmol L^{-1}) and v is scan rate of potential scan (V s^{-1}). The EASA values for each electrode can be calculated from the slope of I_p vs $v^{1/2}$. The EASA values of the GCE, GO/GCE and Cu–Zn/GO/GCE were obtained as 0.0493, 0.1590 and 0.282 cm^2, respectively. These values of EASA for all electrodes proved that an improvement of surface area was obtained after the modification of Cu–Zn/GO on the GCE surface. Therefore a sensitive electrochemical sensor was prepared with high EASA of GO and tremendous properties of metallic Cu and Cu–Zn oxides.

3.2 Electrochemical Oxidation Behavior of Bisphenol A at Different Electrodes

The electrochemical oxidation behaviors of bare GCE, GO/GCE, Cu–GO/GCE, Zn–GO/GCE, Cu–Zn/GO/

 © 2019 Wiley-VCH Verlag GmbH & Co. KGaA, Weinheim

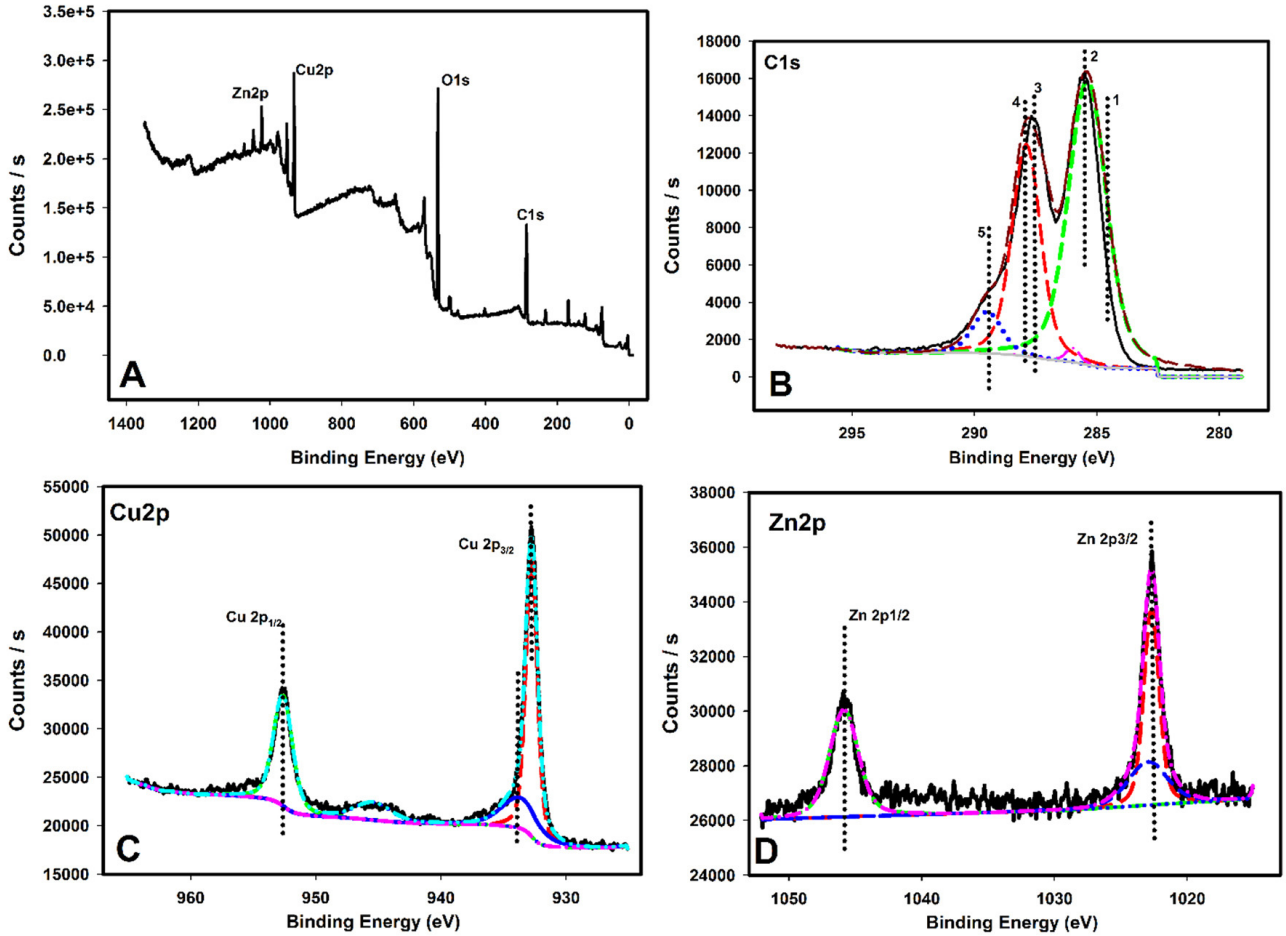

Fig. 2. **(A)** XPS survey spectrum of Cu–Zn/GO/GC composite electrode; core level spectra of **(B)** C 1s, **(C)** Cu 2p and **(D)** Zn 2p.

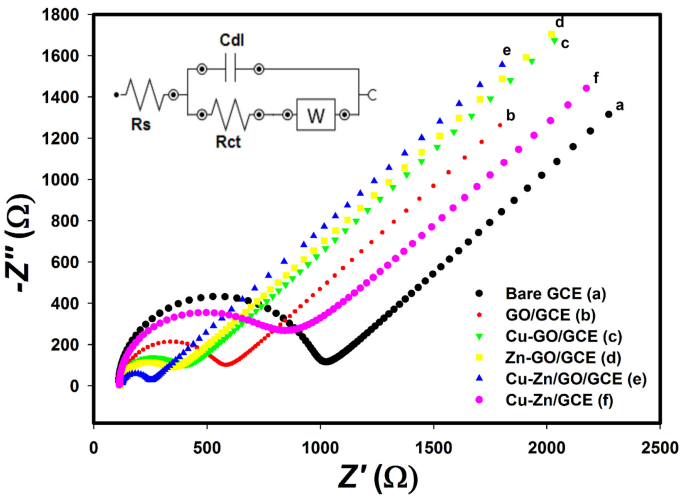

Fig. 3. The representative impedance spectrums of **a)** bare GCE, **b)** GO/GCE, **c)** Cu–GO/GCE, **d)** Zn–GO/GCE, **e)** Cu–Zn/GO/GCE and **f)** Cu–Zn/GCE in the presence 5.0 mmol L^{-1} $K_3[Fe(CN)_6]/K_4[Fe(CN)_6]$ + 0.1 M KCl with the frequencies swept from 0.05 to 75.0×10^3 Hz at the formal potential. Inset is the Randles circuit model for the modified electrodes.

GCE and Cu–Zn/GCE were investigated using CV technique in the BR buffer solution (pH of 7.1) both with and without BPA with a scan rate of 0.05 V s^{-1}. In the absence of BPA, no signals were obtained in the selected potential range at the bare GCE and all modified GCEs (Figure 4A). After the addition of 0.1 mmol L^{-1} BPA in the cell, a well-defined oxidation peak at bare GCE, GO/GCE, Cu–GO/GCE, Zn–GO/GCE, Cu–Zn/GO/GCE and Cu–Zn/GCE (located at about 0.62 V, 0.55 V, 0.56 V, 0.58 V, 0.57 V and 0.53 V, respectively) was observed during the anodic sweep demonstrating a typical irreversible electrode reaction of BPA at the all electrodes (Figure 4B). This irreversible oxidation reaction is in accordance with previous reports [9,11–13]. Since the weak adsorption of BPA to the bare GCE surface leads to slow electron transfer, the oxidation signal of BPA on the bare GCE surface is poor (Figure 4B-a or inset). Unlike the bare GCE, stronger oxidation peaks were obtained on the all metal oxide-graphene oxide composite electrodes. As in the case for GO/GCE, Cu-GO/GCE, Zn–GO/GCE, Cu–Zn/GO/GCE and Cu–Zn/GCE, about 4.27, 7.00, 7.60, 17.3 and 4.41 times larger oxidation peak currents for BPA electrooxidation were obtained when compared to the bare GCE. The increase in the anodic current is

 © 2019 Wiley-VCH Verlag GmbH & Co. KGaA, Weinheim

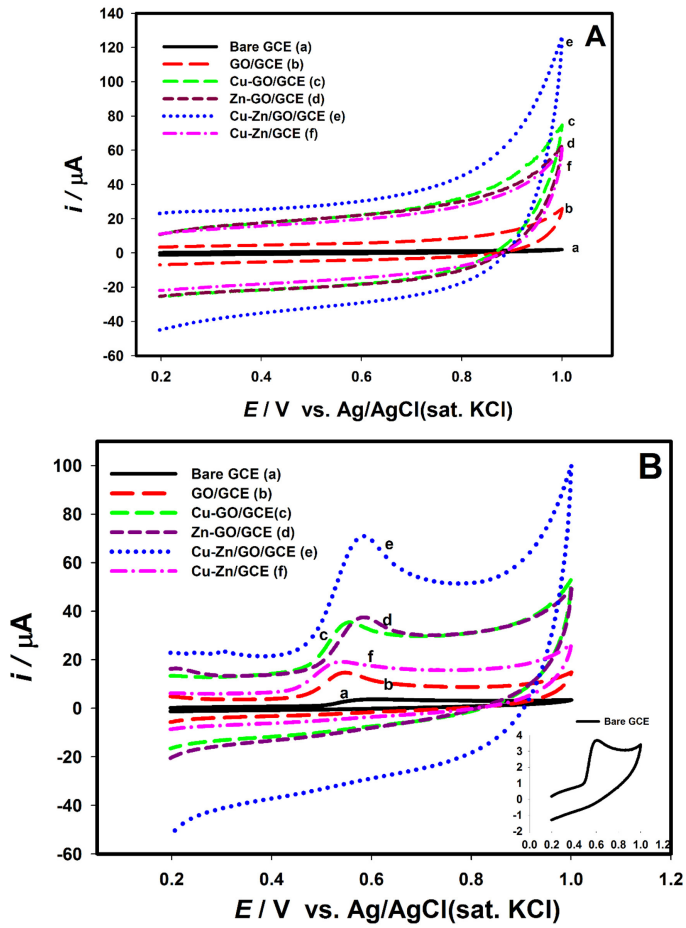

Fig. 4. The cyclic voltammograms obtained for different electrodes in pH 7.1 BR buffer solution **(A)** absence and **(B)** presence of 0.1 mmol L^{-1} BPA with 0.05 V s^{-1} of scan rate: a) bare GCE, **b)** GO/GCE, **c)** Cu–GO/GCE, **d)** Zn–GO/GCE, **e)** Cu–Zn/GO/GCE and **f)** Cu–Zn/GCE.

associated with the higher surface area of the modified electrode and good conductivity provided by metallic Cu, copper oxides and zinc oxides. These observations indicated that the Cu–Zn/GO/GCE served a surface for sensitive determination of BPA.

Additionally, the oxidation peak current of 0.1 mmol L^{-1} BPA decreased with the successive potential scan on the bare GCE in BR buffer solution (Figure 5A). This situation can be due to the adsorbed BPA oxidation product and the polymerization of BPA on the electrode surface (which blocks electrode surface and obstructs further oxidation of BPA) which is in accordance with previous studies [10,19,42–44]. Interestingly, in the case of GO modification on GCE surface, the voltammetric signal of 0.1 mmol L^{-1} BPA decreased by 7.2% after 10 subsequent potential cycles (Figure 5B). The oxidation current of BPA decreased by 20% even after thirty cycles. The same decrease in the BPA oxidation current was also observed on the Cu–Zn/GO/GCE electrode (Figure 5C). As can be seen from the subsequent sweeps, the oxidation peak currents reduced by 6.5% after 10 cycles, 16% after 20 cycles and 21.2% after 30 cycles. According to results, the GO modified electrodes effectively prevent the surface fouling effect caused by the oxidation products of the BPA. These results are in good agreement with the former study reported by Raj and John for electrochemically reduced graphene oxide modified GCE during the detection of uric acid, xanthine, hypoxanthine and caffeine [45]. In another study, Yang et al. were prepared β-cyclodextrin dimer-functionalized multi-walled carbon nanotube for the simultaneous analysis of three phenols (4-aminophenol, 4-AP; 4-chlorophenol, 4-CP; 4-nitrophenol, 4-NP) and the developed electrode surface prevent the surface fouling again [46]. According to the results above, the developed Cu–Zn/GO modified GCE is a suitable platform for the BPA analysis with good stability and repeatability.

3.3 Optimization of Cu–Zn/GO Modified GCE Fabrication

In order to obtain maximum signal for the BPA oxidation, the parameters related with electrodeposition step such as; $CuSO_4$, $ZnSO_4$ concentration (C_{CuSO4} (mmol L^{-1})/C_{ZnSO4} (mmol L^{-1})), deposition time (t_{dep}), deposition potential (E_{dep}) and the GO suspension volume added on the GCE surface were optimized with aid of cyclic voltammetry. The influences of these parameters on the peak current of 0.1 mmol L^{-1} BPA in pH 7.1 BR buffer solution were shown in Figure S1–4 (See supplementary material). The maximum signal was obtained by using 1.0 mmol L^{-1} $CuSO_4$, 1.0 mmol L^{-1} $ZnSO_4$, 300 seconds and −1.4 V and 10 µL of GO.

3.4 Influence of Supporting Electrolyte pH

The effect of supporting electrolyte pH on BPA oxidation is an important issue due to the proton dependent BPA electrooxidation mechanism. The effect of the supporting electrolyte pH was examined in the range of 2.0 to 11.3 by using BR buffer solutions and anodic peak potential (E_{pa}) and anodic peak current (I_{pa}) of the 0.1 mmol L^{-1} BPA were assessed with cyclic voltammetry (Figure 6A). In the studied pH range, E_{pa} of BPA shifted to more negative values with the increase of pH due to the deprotonation reaction of BPA on Cu–Zn/GO/GCE. As can be seen from Figure 5B, the curve obtained between E_{pa} and pH showed a good linearity with a high correlation coefficient (Epa (V) = −0.0594 pH + 0.9913, R^2 = 0.9975). A shift of typically 59.4 mV per pH unit is close to the theoretical Nernst theoretical value of 59.10 mV pH^{-1}. This value indicated that the electrochemical oxidation of BPA occurred by giving the equal number of electrons and protons on the modified electrode. Moreover, I_{pa} values of BPA reached to its maxima at pH 7.1 as pH increases from 2.0 to 11.3. In addition, I_{pa} gradually decreased from pH 7.1 to 11.3, (Figure 6B). As a result, the pH of BR buffer solution was selected as pH 7.1 which is the highest oxidation peak current for determination of BPA with

 © 2019 Wiley-VCH Verlag GmbH & Co. KGaA, Weinheim

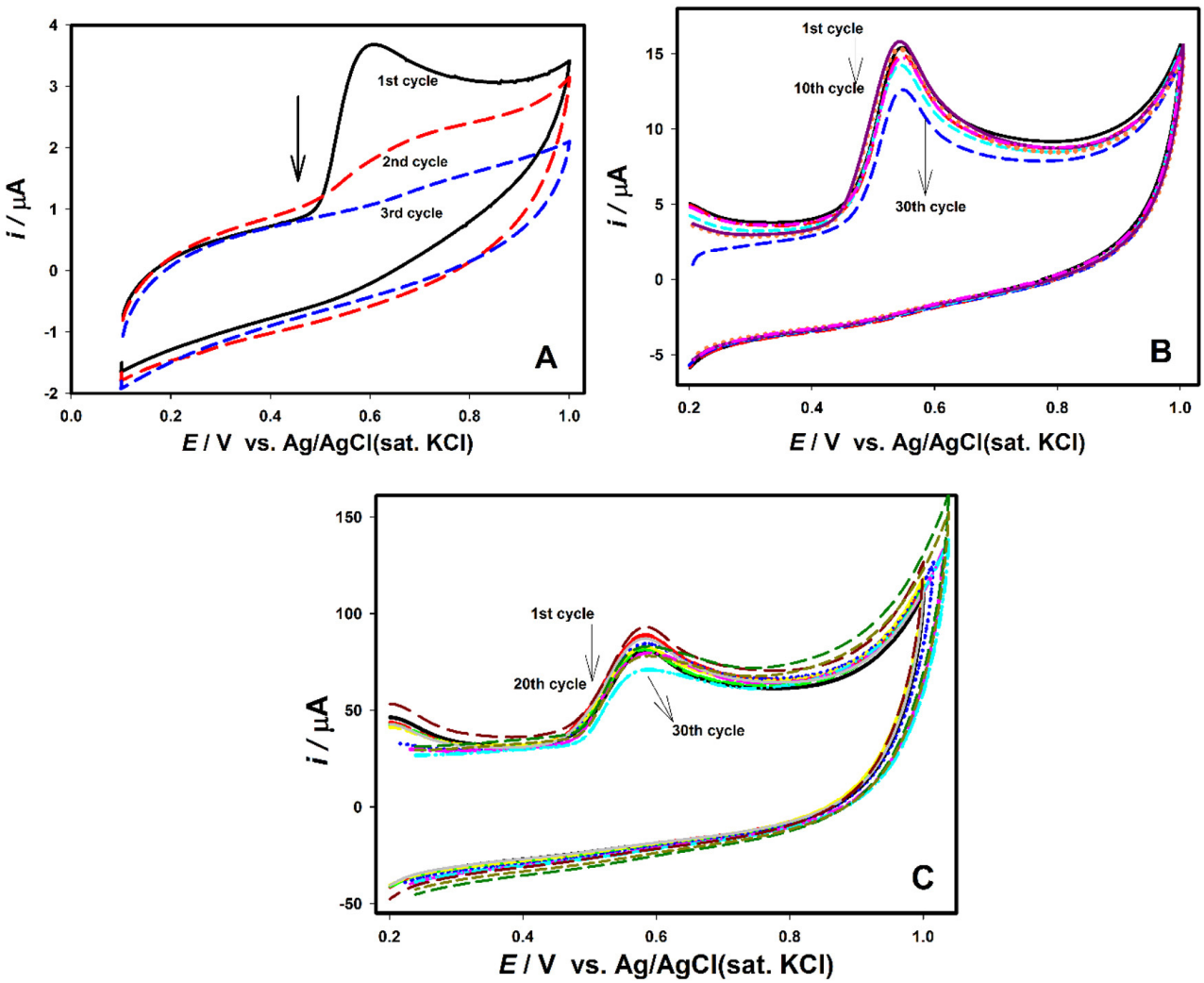

Fig. 5. Successive cyclic voltammograms of 0.1 mmol L^{-1} BPA in pH 7.1 BR buffer at **A)** bare GCE, **B)** GO/GCE and **C)** Cu–Zn/GO/GCE with 0.05 V s^{-1} of scan rate.

high sensitivity. This phenomenon can be elucidated by the fact that the supporting electrolyte pH can affect the present form of BPA. When the pH of the buffer solution was smaller than 9.0 (pKa of BPA: 9.73), BPA is neutral. For the higher pH's BPA is dissociated and present in ionic form. The adsorption of BPA on the electrode surface is occurred easily when the BPA is its neutral form [47,48].

3.5 Effect of Potential Scan Rate

In order to obtain more information about the reaction kinetics of BPA oxidation on Cu–Zn/GO/GC electrode surface, CVs were recorded in pH 7.1 BR solution absence (Figure 7A) and presence (Figure 7B) of 0.1 mmol L^{-1} BPA at different scan rate (5.0–150.0 mV s^{-1}). As can be seen from Figure 7A, well-defined reversible redox peaks were observed at all scan rates in the absence of BPA. The oxidation peak potential has shifted to more positive potentials with the increasing of scan rate. The reversible redox peaks, which did not interfere with the determination peak of BPA in the working potential range, may due to the conversion between hydroxyl and carboxyl groups on the graphene oxide surface [49,50]. With the addition of 0.1 mmol L^{-1} BPA, oxidation peak of BPA was observed at about 0.5 V. From the cyclic voltammograms, the linear curve was obtained between anodic peak currents (I_{pa}) of BPA and the square root of scan rate ($v^{1/2}$) with the expressed equations ($I_{pa}=3.1112\ v^{1/2}+12.5$, $R^2=0.9968$) (Figure 7B). The diffusion-controlled oxidation of BPA on Cu–Zn/GO/GC electrode can be easily understood from the linearity of this curve. Additionally, the E_{pa} of BPA on Cu–Zn/GO/GCE shifted to more positive peak potentials potential scan rate is increased. A linear relationship formed between the oxidation potentials (E_{pa}) and ln v ($E_{pa}=0.054\ ln\ v+0.4245$, $R^2=0.9972$) (Figure 7C). E_{pa} is de-

 © 2019 Wiley-VCH Verlag GmbH & Co. KGaA, Weinheim

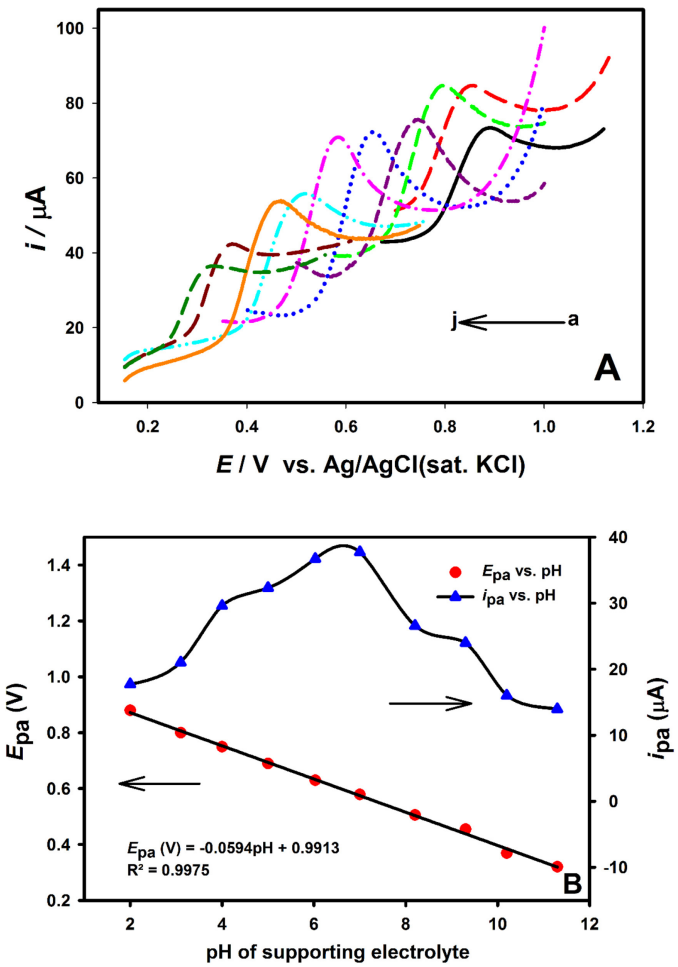

Fig. 6. **A)** Cyclic voltammograms of 1.0 mmol L^{-1} BPA at Cu–Zn/GO/GCE in BR buffer solution with different pH from 2.0 to 11.3: **a)** 2.0, **b)** 3.1, **c)** 4.0, **d)** 5.0, **e)** 6.03, **f)** 7.0, **g)** 8.2, **h)** 9.3000, **i)** 10.2 and **j)** 11.3, **B)** effects of pH value on the current and potential response of 0.1 mmol L^{-1} BPA, with 0.05 V s^{-1} of scan rate.

scribed by the Laviron's equation [51] for an irreversible reaction (Eq. 2);

$$E_p = E^{0'} + \frac{RT}{anF} lnv \quad (2)$$

Where $E^{0'}$ is the formal potential (V), E_p is the peak potential (V), R is the universal gas constant (8.314 J K^{-1} mol^{-1}), α is the charge transfer coefficient for the oxidation reaction, T is the temperature (K), F is the Faraday constant (96,485 C mol^{-1}) and n is the number of electrons in the electrode reaction. The slope of the E_{pa}-ln v line is expressed as RT/anF. According to Bard and Faulkner [52], E_{pa} positively shifted by an amount $1.15RT/\alpha F$ (or $30/\alpha$ mV at 25 °C) for each ten-fold increase in v. Therefore the value of α can be calculated from this equation as 0.24. The transferred electron number (n) in the BPA oxidation reaction was found as 1.98 (approximately equal to 2). So, the proposed electrooxidation mechanism of BPA on the Cu–Zn/GO/GCE surface may be expressed with the Scheme 1, where two electrons and two protons participate in the electrode reaction, which is consistent with other published papers [4,47,48].

3.6 Analytical Performance of Cu–Zn/GO/GCE towards BPA Detection

In order to investigate the analytical performance of the Cu–Zn/GO/GCE for the BPA determination, square-wave voltammetry (SWV) was used in pH 7.1 BR buffer solution. The influence of the SWV parameters (frequency, amplitude, accumulation time and potential) on the electrooxidation peak current of BPA was also investigated in pH 7.1 BR buffer solution containing 5.0 µmol L^{-1} BPA. The effects of these parameters on the peak current of 5.0 µmol L^{-1} BPA in pH 7.1 BR buffer solution were shown in Figure S5–8 (See supplementary material). Optimum parameters were obtained as follows 20 Hz, 0.05 V, 90 sec. and 0.3 V. At the optimum conditions, the SWVs were recorded for BPA oxidation with the concentration range from 3.0 nmol L^{-1} to 20 µmol L^{-1} (Figure 8A). The anodic peak currents (Ipa) of BPA were found to be proportional to its concentration over two linear ranges 3.0 nmol L^{-1}–0.1 µmol L^{-1} (Figure 8B) and 0.35 µmol L^{-1}–20.0 µmol L^{-1} (Figure 8C) with linear regression equations of i_{pa} (µA) = 21.788 C_{BPA} (µmol L^{-1}) + 0.787 (R^2 = 0.9969) and i_{pa} (µA) = 1.2411 C_{BPA} (µmol L^{-1}) + 6.2412 (R^2 = 0.9956), respectively (Figure 8-inset). The limit of detection (LOD) of BPA oxidation on Cu–Zn/GO modified GCE was calculated as 0.88 nmol L^{-1} with the equation LOD = 3.3 σ/m, (σ: the standard deviation of the response for supporting electrolyte, m: the calibration graph' slope). In addition, a comparison of different electrochemical methods and present method for the determination of BPA done and listed in Table 1. As can be seen from the table, the novel electrode, Cu–Zn/GO/GCE, developed for the BPA determination has higher

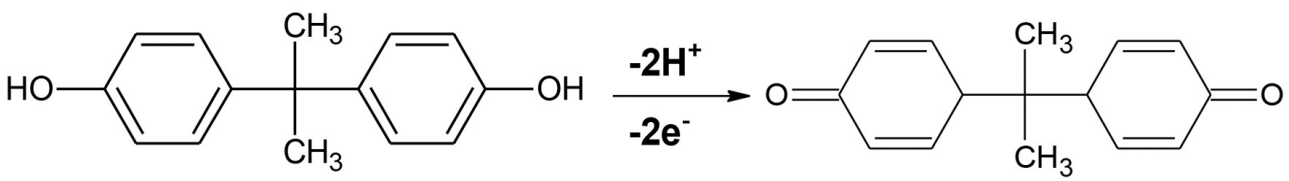

Scheme 1. The possible oxidation mechanism of BPA at Cu–Zn/GO/GC electrode.

 © 2019 Wiley-VCH Verlag GmbH & Co. KGaA, Weinheim

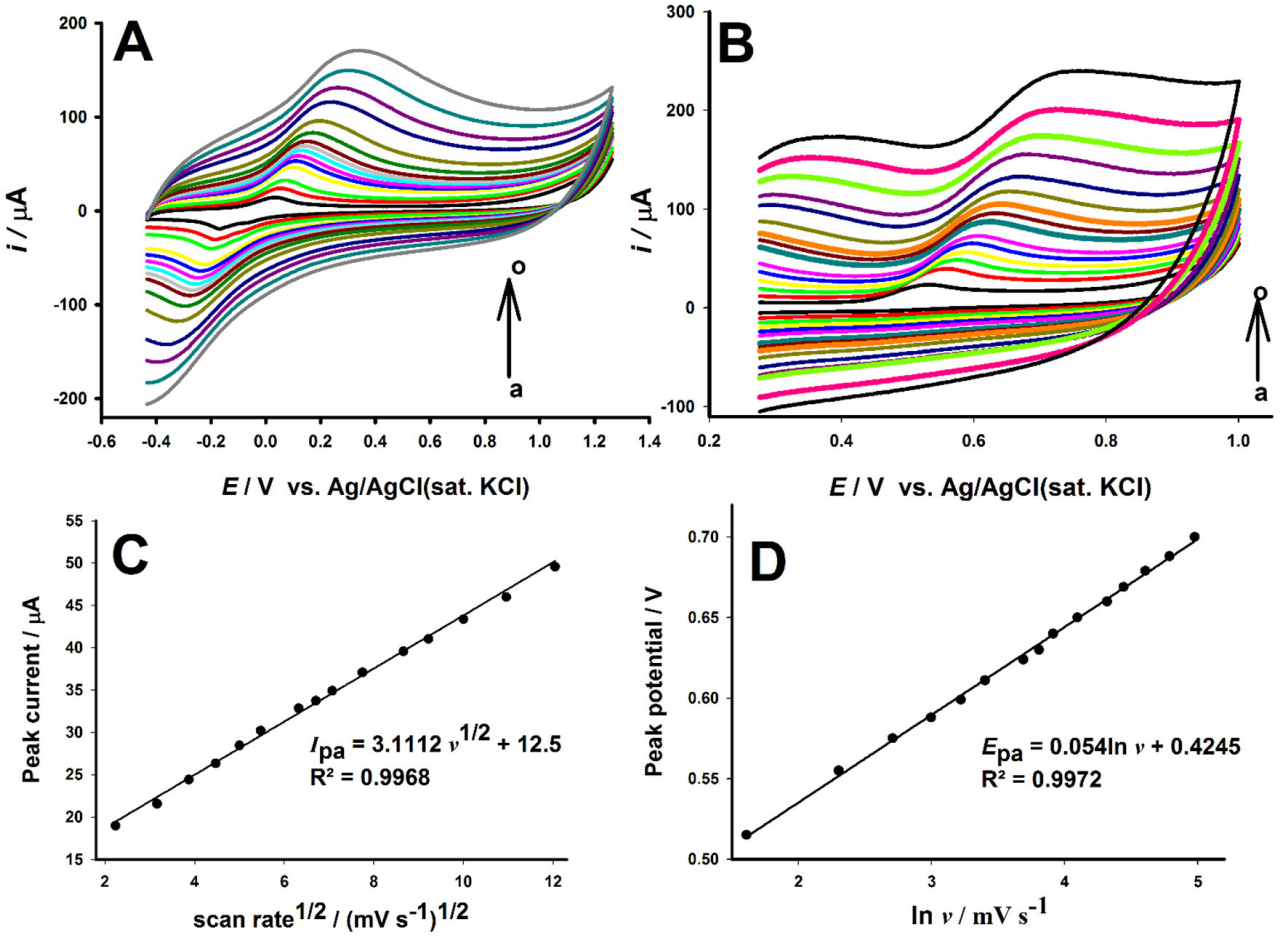

Fig. 7. Cyclic voltammograms **A)** absence and **B)** presence of 0.1 mmol L^{-1} BPA at Cu–Zn/GO/GCE with different scan rates (a–o: 5.0–145.0 mV s^{-1}), **C)** the plots of oxidation peak current of BPA versus the square root of scan rate, **D)** the relationship between peak potential and ln *v*.

sensitivity and lower detection limit than some reported studies.

3.7 Reproducibility and Long-time Stability

To assess the reproducibility of the Cu–Zn/GO/GCE, the responses of five different composite electrodes prepared with the same procedures towards BPA oxidation were recorded for inter-day (n = 5) and intra-day (n = 5) measurements. The relative standard deviations (RSD) values were calculated from the SWV analyses for inter-day and intra-day (2.0 µmol L^{-1} BPA in pH 7.1 BR buffer solution) as 4.55 % and 5.65 %, respectively (Figure S9A–B-See supplementary material). This evaluation indicated that the composite electrode has a good reproducibility.

The long-time stability of the Cu–Zn/GO/GCE was also examined by evaluating peak current of 2.0 µmol L^{-1} BPA. The Cu–Zn/GO/GCE was kept at standard conditions in pH 7.1 BR buffer solution during the long-time stability studies. The oxidation peak current of 2.0 µmol L^{-1} BPA on Cu–Zn/GO/GCE decreased less than 7.5 % from their original values even after the 8 days. These studies proved that the Cu–Zn/GO/GCE stability was good enough as a long-time voltammetric sensor (Figure S10 – See supplementary material).

3.8 Interference Studies

Selectivity of the developed electrode towards the target molecule is an important parameter in voltammetric applications. For this purpose, to investigate of the Cu–Zn/GO/GCE selectivity towards BPA, the effect of potentially interfering substances were studied by examining for the response of 2.0 µmol L^{-1} BPA in pH 7.1 BR buffer solution with SWV. At the optimum conditions, two thousand-fold concentration of K^+, Na^+, Cl^-, Ba^{+2}, Mg^{+2}, Ca^{+2}, Al^{3+}, Zn^{2+}, Ni^{+2}, Pb^{2+}, Cd^{+2}, CH_3COO^-, NH_4^+, $C_2O_4^{2-}$, NO_3^- and SO_4^{2-} has no significant interference on the 2.0 µmol L^{-1} BPA signal since less than % 5.0 change in peak current was observed. An increase in peak current in the presence of more than 50-fold amount of Fe^{3+} and 500-fold amount of Cu^{2+} ion was observed. Other potential electroactive organic interferences which may be present in plastic samples such as glucose (GLU),

 © 2019 Wiley-VCH Verlag GmbH & Co. KGaA, Weinheim

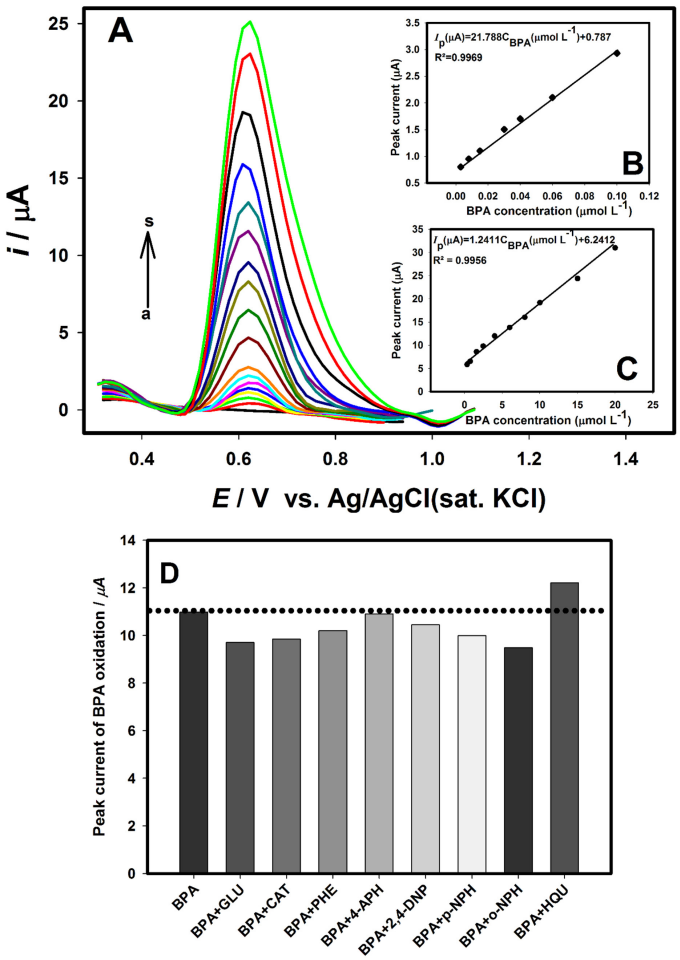

Fig. 8. **A)** Square wave voltammograms with different concentrations of BPA (a–s: 3.0 nmol L^{-1} to 20 μmol L^{-1}) in the pH 7.1 BR buffer solution at Cu–Zn/GOGCE. *Inset:* two linear curves of oxidation peak current versus different concentrations of BPA **B)** 3.0 nmol L^{-1}–0.1 μmol L^{-1} and **C)** 0.35 μmol L^{-1}–20.0 μmol L^{-1}, **D)** Interference studies of the developed Cu–Zn/GO/GC electrode for the 2.0 μmol L^{-1} BPA only or with 100.0 μmol L^{-1} GLU, CAT, PHE, 4-APH, 2,4-DNP, *p*-NPH, *o*-NPH, HQU, respectively.

catechol (CAT), phenol (PHE), 4-aminophenol (4-APH), 2,4-dinitrophenol (2,4-DNP), *p*-nitrophenol (*p*-NPH), *o*-nitrophenol (*o*-NPH), hydroquinone (HQU) were also investigated. Figure 8D displays that 50-fold concentrations of these compounds have no obvious interference towards the oxidation peak currents of 2.0 μmol L^{-1} BPA, with deviations <10%. These results showed that the developed composite electrode displayed good in selectivity for determination of BPA contents in real samples.

3.9 Analytical Application of the Cu–Zn/GO/GCE

To assess the performance of the developed method in practical analytical applications, the proposed method was applied to baby feeding bottle, pacifier, water bottle and food storage container samples which were prepared according to section 2.4. The contents of BPA in real samples and the recovery results are listed in Table 2. As a result of the measurements, BPA was detected only in the food storage container samples as 0.544 μmol L^{-1}. The contents of BPA in the other samples were all below the LOD. Moreover, the applicability of the method to real samples was also tested with standard additions method under the optimum conditions. The recoveries for the added standards were found in the range of 94.27 and 123.20%. The satisfactory recovery values indicated that Cu–Zn/GO/GCE can be successfully used for the BPA analysis in real samples.

The results for BPA determination in food storage container samples with SWV technique were compared with the UV-vis technique. The statistical comparison of SWV analysis results with UV-vis analysis results was achieved using the t-test and *F*-test. The *t*-test method was applied to compare the average values for the BPA determination by the two techniques. The calculated t_t was 0.035 ($p > 0.05$), which was lower than the theoretical value t_c of 2.77. These results revealed that there is no systematic difference between the results of the two methods. The discrepancy between the data obtained from SWV with Cu–Zn/GO/GCE and the UV-vis method was confirmed by applying the *F*-test. The *F* value obtained from determination of BPA in the food storage container samples ($F_t = 1.45$) was lower than the theoretical F value ($F_c = 19.0$) at the 95% confidence level, demonstrating that there is no significant difference between the two methods. The t-test and F-test results indicated that the novel method offers accurate, precise and reliable data for BPA detection in real samples.

4 Conclusions

In this study, a cost and time-effective, easy, sensitive, selective and reliable voltammetric technique was suggested for BPA determination using the unique properties of Cu^0–CuO, ZnO and GO. The Cu–Zn/GO/GCE was prepared with a simple electrochemical method which showed the best peak current response of BPA oxidation. The SWV results displayed that the peak currents of BPA oxidation were found to be proportional to its concentration over two linear ranges 3.0 nmol L^{-1}-0.1 μmol L^{-1} and 0.35 μmol L^{-1}–20.0 μmol L^{-1} and with 0.88 nM of detection limit on Cu–Zn/GO/GCE in pH 7.1 BR buffer solution. As a result of selectivity studies, the developed composite electrode behaved good in selectivity for detection of BPA contents in real samples. Moreover, a good reproducibility and acceptable stability were obtained for BPA determination with the modified electrode. The Cu–Zn/GO/GCE is ideally suited as a fast screening assay to detect and quantify the presence of BPA in baby feeding bottle, pacifier, water bottle and food storage container samples. By taking all results it can be concluded that the novel method will offer a great promise for the determination of BPA in real samples with high selectivity and reproducibility.

 © 2019 Wiley-VCH Verlag GmbH & Co. KGaA, Weinheim

Table 1. Comparison of different modified electrodes for BPA determination.

Electrodes	Mode	LR (mol L^{-1})	LOD (mol L^{-1})	Sample	Ref.
c-MWCNT/GCE	LSV	1.0×10^{-7}–1.0×10^{-5}	2.0×10^{-8}	Food package	[16]
PGA/MWCNT-NH_2	DPV	1.0×10^{-8}–1.0×10^{-6}	2.0×10^{-8}	Plastic or paper products	[15]
CMK-3/nano-CILPE	LSV	2.0×10^{-7}–2.0×10^{-6}	1.5×10^{-4}	Drinking bottle, plastic bag	[48]
Gr–AuCu	LSV	1.0×10^{-7}–1.0×10^{-4}	1.31×10^{-6}	–	[13]
Gr–AgCu		1.0×10^{-7}–3.0×10^{-5} 3.0×10^{-5}–1.0×10^{-4}	1.91×10^{-6}		
Carbon nanotube/ionic liquid/titania/Nafion	DPV	1.0×10^{-9}–1.0×10^{-5}	5.0×10^{-10}	Food package, water bottles	[14]
AuPdNPs/GNs	DPV	5.0×10^{-8}–1.0×10^{-5}	8.0×10^{-9}	Food package	[9]
MWCNTs/PCV/GCE	DPV	5.0×10^{-8}–1.0×10^{-4}	1.0×10^{-8}	Plastic samples	[21]
Au@PDA/RGO	DPV	1.25×10^{-8}–3.68×10^{-6}	1.0×10^{-10}	Plastic products	[12]
AuNPs-rGO-MWCNTs/GCE	DPV	5.0×10^{-9}–1.0×10^{-7} 1.0×10^{-7}–2.0×10^{-5}	1.0×10^{-9}	River water, shopping receipt samples	[11]
GO–CNTs/Fe_3O_4/PGA/GCE	DPV	3.0×10^{-9}–2.0×10^{-7} 2.0×10^{-7}–3.0×10^{-5}	1.0×10^{-9}	Mineral water bottles, PVC food packeges	[17]
Poly(CTAB)/MWCNTs/PG	SWV	2.0×10^{-9}–8.0×10^{-7}	1.34×10^{-10}	Plastic drinking bottle	[3]
Ti/TiO_2/MIFs	CA	4.4×10^{-9}-1.3×10^{-4}	1.3×10^{-9}	Seawater, paper cup samples	[24]
Cu–Zn/GO/GCE	SWV	3.0×10^{-9}–1.0×10^{-7} 3.5×10^{-7}–2.0×10^{-5}	8.8×10^{-10}	baby feeding bottle, pacifier, water bottle and food storage container samples	This study

c-MWCNT/GCE: carboxylated multi-walled carbon nanotubes modified glassy carbon electrode; MWCNT-MAM/GCE:MWCNT melamine complex on GCE; LSV: Linear sweep voltammetry; PGA/MWCNT-NH_2: polyglutamate acid/amino-functionalised MWCNT; DPV: differential pulse voltammetry; CMK-3/nano-CILPE: ordered mesoporous carbon CMK-3 modified nano-carbon ionic liquid paste electrode; AuNPs/MWCNT/GCE: Au nanoparticles modified MWCNT/GCE; Gr–AuCu: Graphene AuCu bimetallic composite; Gr–AgCu: Gr–AuCu: Graphene AgCu bimetallic composite; AuPdNPs/GNs: AuPd-nanoparticles-loadedgraphene nanosheets; MWCNTs/PCV/GCE: MWCNTs-poly crystal violet modified GCE; Au@PDA/RGO: Au nanoparticles polydopamine functionalized reduced graphene oxide, Poly(CTAB)/MWCNTs/PGE: poly(cetyltrimethylammonium) bromide/MWCNTs/pencil graphite electrode; Ti/TiO_2/MIFs: Ti/TiO_2/molecularly imprinting films; CA: Charonoamperometry.

Table 2. Determination of BPA in various plastic samples (n = 3).

Samples	Added (μmol L^{-1})	Found (μmol L^{-1})		Recovery (%)		RSD (%)	
		SWV	UV-vis	SWV	UV-vis	SWV	UV-vis
Baby feeding bottle	0	nd	nd	–	–	–	–
	1.0	0.964	1.085	96.40	108.50	1.25	3.41
	4.0	4.235	3.991	105.88	99.78	3.41	4.43
	8.0	8.823	7.541	110.28	94.27	1.12	3.76
Pacifier	0	nd	nd	–	–	–	–
	1.0	0.971	1.121	97.00	112.10	4.21	2.52
	4.0	4.121	3.987	103.03	99.68	3.82	3.12
	8.0	7.789	8.324	97.36	104.05	2.95	4.51
Water bottle	0	nd	nd	–	–	–	–
	1.0	1.135	1.232	113.5	123.20	2.21	4.87
	4.0	3.976	4.213	99.40	105.33	3.45	3.67
	8.0	8.412	8.232	105.15	102.90	2.87	4.62
	0	0.544	0.523	–	–	4.61	3.83
Food storage container	1.0	1.603	1.541	103.82	101.18	0.31	2.02
	4.0	4.612	4.501	101.49	99.51	1.55	2.74
	8.0	8.351	8.612	97.74	101.04	3.85	2.77

Acknowledgments

This work was supported by the Ege University Research Funds (BAP Project No: 17 FEN 073). The author would like to thank Prof. Dr. Zekerya Dursun for his valuable contributions to this study.

References

[1] Y. T. Yaman, S. Abacı, *Sensors* **2016**, *16*, 756.
[2] R. Wannapob, P. Thavarungkul, S. Dawan, A. Numnuam, W. Limbut, P. Kanatharana, *Electroanalysis* **2017**, *29*, 472.
[3] G. Bolat, Y. T. Yaman, S. Abaci, *Sens. Actuators B: Chem.* **2018**, *255*, 140.
[4] J. Zhang, X. Xu, Z. Chen, *Ionics* **2018**, https://doi.org/10.1007/s11581-018-2462-1.

 © 2019 Wiley-VCH Verlag GmbH & Co. KGaA, Weinheim

[5] A. L. Heffernan, K. Thompson, G. Eaglesham, S. Vijayasarathy, J. F. Mueller, P. D. Sly, M. J. Gomez, *Talanta* **2016**, *151*, 224.
[6] Z. Zhang, S. M. Rhind, C. Kerr, M. Osprey, C. E. Kyle, *Anal. Chim. Acta* **2011**, *685*, 29.
[7] S. Wang, X. Wei, L. Du, H. Zhuang, *Luminescence* **2005**, *46*, 46.
[8] G. Liu, Z. Chen, X. Jiang, D. Feng, J. Zhao, D. Fan, W. Wang, *Sens. Actuators B: Chem.* **2016**, *228*, 302.
[9] B. Su, H. Shao, N. Li, X. Chen, Z. Cai, X. Chen, *Talanta* **2017**, *166*, 126.
[10] A. Ghanam, A. A. Lahcen, A. Amine, *J. Electroanal. Chem.* **2017**, *789*, 58.
[11] Y. Hao, F. Xiao, C. Xiao-xia, Q. Jin-li, G. Xiao-ling, X. Na, G. Lou-jun, *J. Electroanal. Chem.* **2017**, *45*, 713.
[12] X. Xu, Q. Zheng, G. Bai, L. Song, Y. Yao, X. Cao, S. Liu, C. Yao, *Electrochim. Acta* **2017**, *242*, 56.
[13] F. Pogacean, A. R. Biris, C. Socaci, M. Coros, L. Magerusan, M. C. Rosu, M. D. Lazar, G. Borodi, S. Pruneanu, *Nanotechnology* **2016**, *27*, 484001.
[14] J. Jang, D. Kim, W. Lee, *Anal. Lett.* **2016**, *49*, 2018.
[15] Y. Lin, K. Liu, C. Liu, L. Yin, Q. Kang, L. Li, B. Li, *Electrochim. Acta* **2014**, *133*, 492.
[16] J. Li, D. Kuang, Y. Feng, F. Zhang, M. Liu, *Microchim. Acta* **2011**, *172*, 379.
[17] K. Deng, X. Liu, C. Li, Z. Hou, H. Huang, *Anal. Methods* **2017**, *9*, 5509.
[18] M. Wang, Y. Shi, Y. Zhang, Y. Wang, H. Huang, J. Zhang, J. Song, *Electroanalysis* **2017**, *29*, 2620.
[19] E. R. Santana, C. A. De Lima, J. V Piovesan, A. Spinelli, *Sens. Actuators B: Chem.* **2017**, *240*, 487.
[20] H. Ezoji, M. Rahimnejad, M. Asghary, *Pak. J. Biotechnol.* **2016**, *13*, 133.
[21] W. Wang, J. Tang, S. Zheng, X. Ma, J. Zhu, F. Li, J. Wang, *Food Anal.Methods* **2017**, *10*, 3815.
[22] H. Y. Li, X. L. Wang, Z. X. Wang, W. Jiang, *Russ. J. Electrochem.* **2017**, *53*, 132.
[23] M. Ma, X. Tu, G. Zhan, C. Li, S. Zhang, *Microchim. Acta* **2014**, *181*, 565.
[24] Q. Yang, X. Wu, H. Peng, L. Fu, X. Song, J. Li, H. Xiong, L. Chen, *Talanta* **2018**, *176*, 595.
[25] X. Liu, L. Zhang, S. Wei, S. Chen, X. Ou, Q. Lu, *Biosens. Bioelectron.* **2014**, *57*, 232.
[26] Y. Jun, W. Li, *Biosens. Bioelectron.* **2014**, *56*, 300.
[27] P. Deng, Z. Xu, Y. Kuang, *Food Chem.* **2014**, *157*, 490–497.
[28] J. Zou, Z. Liu, C. Dong, *Anal. Methods* **2016**, *9*, 134.
[29] Y. Zhang, X. Sun, L. Zhu, H. Shen, N. Jia, *Electrochim. Acta.* **2011**, *56*, 1239.
[30] S. Muralikrishna, K. Sureshkumar, T. S. Varley, D. H. Nagaraju, T. Ramakrishnappa, *Anal. Methods* **2011**, *6*, 8698.
[31] H. Nolan, B. Mendoza-Sánchez, N. A. Kumar, N. McEvoy, V. Nicolosi, G. S. Duesberg, *Phys. Chem. Chem. Phys.* **2014**, *16*, 2280.
[32] S. U. Karabiberoglu, Z. Dursun, *J. Electroanal. Chem.* **2018**, *815*, 76.
[33] M. Devaraj, R. Saravanan, R. Deivasigamani, V. K. Gupta, F. Gracia, S. Jayadevan, *J. Mol. Liquids* **2016**, *221*, 930.
[34] N. Cioffi, L. Torsi, N. Ditaranto, G. Tantillo, L. Ghibelli, L. Sabbatini, T. Bleve-Zacheo, M. D′Alessio, P. G. Zambonin, E. Traversa, *Chem. Mater.* **2005**, *17*, 5255.
[35] A. C. Tavares, M. I. S. Pereira, M. H. Mendonça, M. R. Nunes, F. M. Costa, C. M. Sa, *J. Electroanal. Chem.* **1998**, *449*, 91.
[36] S. Chen, L. Brown, M. Levendorf, W. Cai, S. Y. Ju, J. Edgeworth, X. Li, C. W. Magnuson, A. Velamakanni, R. D. Piner, J. Kang, J. Park, R. S. Ruoff, *ACS Nano* **2011**, *5*, 1321.
[37] X. Ke, G. Zhu, Y. Dai, Y. Shen, J. Yang, J. Liu, *J. Electroanal. Chem.* **2018**, *817*, 176.
[38] S. Ameen, M. S. Akhtar, H. S. Shin, *Talanta* **2012**, *100*, 377.
[39] J. Bai, J. C. Ndamanisha, L. Liu, L. Yang, L. Guo, *J. Solid State Electrochem.* **2010**, *14*, 2251.
[40] M. J. Song, S. W. Hwang, D. Whang, *Talanta* **2010**, *80*, 1648.
[41] S. J. Konopka, B. Mcduffie, *Anal. Chem.* **1970**, *42*, 1741.
[42] H.-shun Yin, Y.-lei Zhou, S.-yun Ai, *J. Electroanal. Chem.* **2009**, *626*, 80.
[43] M. F. Brugnera, M. A. G. Trindade, M. V. B. Zanoni, *Anal. Lett.* **2010**, *43*, 2823.
[44] G. F. Pereira, L. S. Andrade, R. C. Rocha-Filho, N. Bocchi, S. R. Biaggio, *Electrochim. Acta* **2012**, *82*, 3.
[45] M. A. Raj, S. A. John, *Anal. Chim. Acta* **2013**, *771*, 14.
[46] L. Yang, S. Fan, G. Deng, Y. Li, X. Ran, H. Zhao, C. Peng Li, *Biosens. Bioelectron.* **2015**, *68*, 617.
[47] Y. Huang, X. Li, S. Zheng, *Talanta* **2016**, *160*, 241.
[48] Y. Li, X. Zhai, X. Liu, L. Wang, H. Liu, H. Wang, *Talanta* **2016**, *148*, 362.
[49] R. Shi, J. Liang, Z. Zhao, Y. Liu, A. Liu, *Sensors* **2018**, *18*, 1660.
[50] S. P. Kumar, R. Manjunatha, C. Nethravathi, G. S. Suresh, M. Rajamathi, T. V. Venkatesh, *Electroanalysis* **2011**, *23*, 842.
[51] E. Laviron, *J. Electroanal. Chem.* **1979**, *100*, 263.
[52] A. J. Bard, L. R. Faulkner, *Electrochemical Methods Fundementals and Application 2nd ed.*, Wiley, **2004**.

Received: June 18, 2018
Accepted: October 19, 2018
Published online on November 13, 2018

 © 2019 Wiley-VCH Verlag GmbH & Co. KGaA, Weinheim